



Research paper

Allocation of freshly assimilated carbon into primary and secondary metabolites after in situ ^{13}C pulse labelling of Norway spruce (*Picea abies*)

Steffen Heinrich^{1,2,5}, Michaela A. Dippold³, Christiane Werner¹, Guido L.B. Wiesenberg⁴, Yakov Kuzyakov³ and Bruno Glaser²

¹Department of Agro-Ecosystem Research, BAYCEER, University of Bayreuth, Universitätsstraße 30, 95448 Bayreuth, Germany; ²Soil Biogeochemistry, Martin-Luther University Halle-Wittenberg, von-Seckendorff-Platz 3, 06120 Halle, Germany; ³Department of Agricultural Soil Science, University of Göttingen, 37077 Göttingen, Germany; ⁴Department of Geography, University of Zurich, CH-8057 Zurich, Switzerland; ⁵Corresponding author (steffen.heinrich@uni-bayreuth.de)

Received February 12, 2015; accepted August 5, 2015; published online September 29, 2015; handling Editor Torgny Näsholm

Plants allocate carbon (C) to sink tissues depending on phenological, physiological or environmental factors. We still have little knowledge on C partitioning into various cellular compounds and metabolic pathways at various ecophysiological stages. We used compound-specific stable isotope analysis to investigate C partitioning of freshly assimilated C into tree compartments (needles, branches and stem) as well as into needle water-soluble organic C (WSOC), non-hydrolysable structural organic C (stOC) and individual chemical compound classes (amino acids, hemicellulose sugars, fatty acids and alkanes) of Norway spruce (*Picea abies*) following in situ ^{13}C pulse labelling 15 days after bud break. The ^{13}C allocation within the above-ground tree biomass demonstrated needles as a major C sink, accounting for 86% of the freshly assimilated C 6 h after labelling. In needles, the highest allocation occurred not only into the WSOC pool (44.1% of recovered needle ^{13}C) but also into stOC (33.9%). Needle growth, however, also caused high ^{13}C allocation into pathways not involved in the formation of structural compounds: (i) pathways in secondary metabolism, (ii) C-1 metabolism and (iii) amino acid synthesis from photorespiration. These pathways could be identified by a high ^{13}C enrichment of their key amino acids. In addition, ^{13}C was strongly allocated into the *n*-alkyl lipid fraction (0.3% of recovered ^{13}C), whereby ^{13}C allocation into cellular and cuticular exceeded that of epicuticular fatty acids. ^{13}C allocation decreased along the lipid transformation and translocation pathways: the allocation was highest for precursor fatty acids, lower for elongated fatty acids and lowest for the decarboxylated *n*-alkanes. The combination of ^{13}C pulse labelling with compound-specific ^{13}C analysis of key metabolites enabled tracing relevant C allocation pathways under field conditions. Besides the primary metabolism synthesizing structural cell compounds, a complex network of pathways consumed the assimilated ^{13}C and kept most of the assimilated C in the growing needles.

Keywords: amino acid pathways, carbohydrate turnover, carbon allocation, compound-specific isotope analysis, lipid biosynthesis, metabolite tracing, photosynthetic partitioning.

Introduction

Carbon (C) and nitrogen (N) cycling in forest ecosystems have been intensively studied during the past decades, especially regarding the expected climate change scenarios. Forest ecosystems contain up to 80% of the above-ground C worldwide

and 40% of the below-ground terrestrial C (Dixon and Turner 1991, Körner 2003), making them either a major sink or source of atmospheric CO_2 depending on environmental conditions (Malhi et al. 1999). About 60% of the total forest C is located in boreal and temperate forest ecosystems, of which ~84% occurs in soil organic matter (Malhi et al. 1999). Höglberg et al.

(2001) showed that recently assimilated C constitutes up to 50% of the CO₂ deriving from soil respiration in forests of the boreal zone. They also demonstrated that the coupling of the photosynthetic activity to soil C efflux is the key determinant of the C budget in these ecosystems. Thus, the mobile C pool, mainly consisting of non-structural carbohydrates such as sucrose, fructose, glucose and starch, is crucial for the C allocation within trees and consequently for the C balance of the entire ecosystem (Würth et al. 2005). In this context, assimilates, especially non-structural carbohydrates, have been studied for several decades in terms of compositional changes and distribution to different plant organs and tissues in many plant species (Hoch et al. 2002, 2003). Nonetheless, our knowledge about C allocation patterns within the plant–soil system—regarding physiological processes such as growth, storage and respiration—is rather patchy (Trumbore 2006).

Short-term ¹³C pulse labelling is a widespread approach to trace the fate of recently assimilated C. Here, whole plants (Lippu 1994, Keel et al. 2006, Sangster et al. 2010, Epron et al. 2011, Glaser et al. 2012) or parts thereof (Nogués et al. 2006, Streit et al. 2013) are exposed to a highly ¹³C-enriched atmosphere, usually for periods ranging from minutes to several hours. This generates strong isotope labelling, which can be detected within the C pools in plants and soil (see review by Epron et al. 2012). These techniques shed new light into many not yet fully understood physiological mechanisms such as phloem loading/unloading including transfer velocities and time lags between C assimilation and respiration (Plain et al. 2009, Kuzyakov and Gavrichkova 2010, Barthel et al. 2011), partitioning of C fluxes to heterotrophic and autotrophic respiration (Kuptz et al. 2011, Biasi et al. 2012) or translocation, storage and remobilization of assimilated C during the season (Kuzyakov and Domanski 2000, Kagawa et al. 2006, Keel et al. 2012). These and further isotope labelling studies traced the isotopic composition of certain plant tissues, non-structural carbohydrates, including soluble sugars and starch, and cellulose as representative of the structural C pool, yielding important insights into fundamental metabolic processes (Keel et al. 2012, Richardson et al. 2013).

Moreover, combining ¹³C pulse labelling with compound-specific ¹³C analyses opens up new horizons in the research on partitioning mechanisms of C between metabolites and metabolic groups, their formation and turnover times (Brüggemann et al. 2011). Isotope application continues to have high potential, especially in quantifying C allocation into individual compound classes (Gao et al. 2012, Streit et al. 2013). It can contribute significantly to expanding our understanding of mechanisms underlying the C allocation processes in plants.

In this study, we explore partitioning of recently assimilated C in Norway spruce (*Picea abies*) under field conditions in a temperate climate (Fichtelgebirge, Germany), 15 days after bud break in May. After 6 h of in situ ¹³CO₂ pulse labelling, we

determined the allocation and incorporation of ¹³C into (i) bulk tissue of various tree compartments and stem segments, (ii) water-soluble organic C (WSOC), which contains especially low molecular weight carbohydrates and acts as a main transport form of C and precursors for many other metabolites, (iii) non-hydrolysable structural organic C (stOC) containing lignin, cellulose and structural proteins and (iv) various compound classes within the needles. We chose four compound classes of different metabolic origin to trace a broad spectrum of metabolic pathways (Figure 1): (i) amino acids, as basic components of protein synthesis, are involved in regulating almost all metabolic processes and also represent important cellular building blocks; (ii) hemicellulose sugars, as structural compounds of primary and secondary cell walls of plants; (iii) fatty acids, as part of oils, fats, epicuticular waxes and membranes, which are also the precursors for alkane synthesis; and (iv) alkanes, as a main component of epicuticular waxes (Jetter et al. 2000). For compound-specific analysis, we focused on fast-responding compound classes that represent short-term C dynamics and thus did not investigate the main structural, highly polymeric pools of cellulose and lignin.

For these compound classes, we hypothesize:

- (i) a high ¹³C allocation into all structural compound classes such as amino acids and hemicelluloses, which are directly involved in cell wall and tissue formation during bud break;
- (ii) a high ¹³C allocation into precursor fatty acids (16:0 and 18:0) and lower allocation into their elongated/decarbonylated follow-up products synthesized for export to the cuticle and wax layer;
- (iii) a similar compound-specific isotope enrichment pattern of cellular and cuticular and into epicuticular lipids due to the formation of extracellular compounds within the epidermal cells.

Materials and methods

Site description

The experiment was conducted in a clearing of a mixed conifer forest (49°52'55"N, 11°36'8"E), close to the city Bayreuth in the north-eastern part of Bavaria, Germany. Norway spruce (*P. abies*) is the dominant tree apart from very few exceptions such as birch (*Betula pendula*), beech (*Fagus sylvatica*) and Black pine (*Pinus nigra*). The study site was situated on a flat slope at 437 m above sea level. Derived from loamy to sandy deposits, soil development resulted in a stagnic cambisol (IUSS Working Group Reference Base 2014). The climate in this region is characterized by long-term mean annual temperature of 8.2 °C and annual precipitation of 740 mm (Kreyling et al. 2012).

Experimental set-up

In May 2009, the experiment was carried out in the early phase of the vegetation period 15 days after bud break. Overall, eight

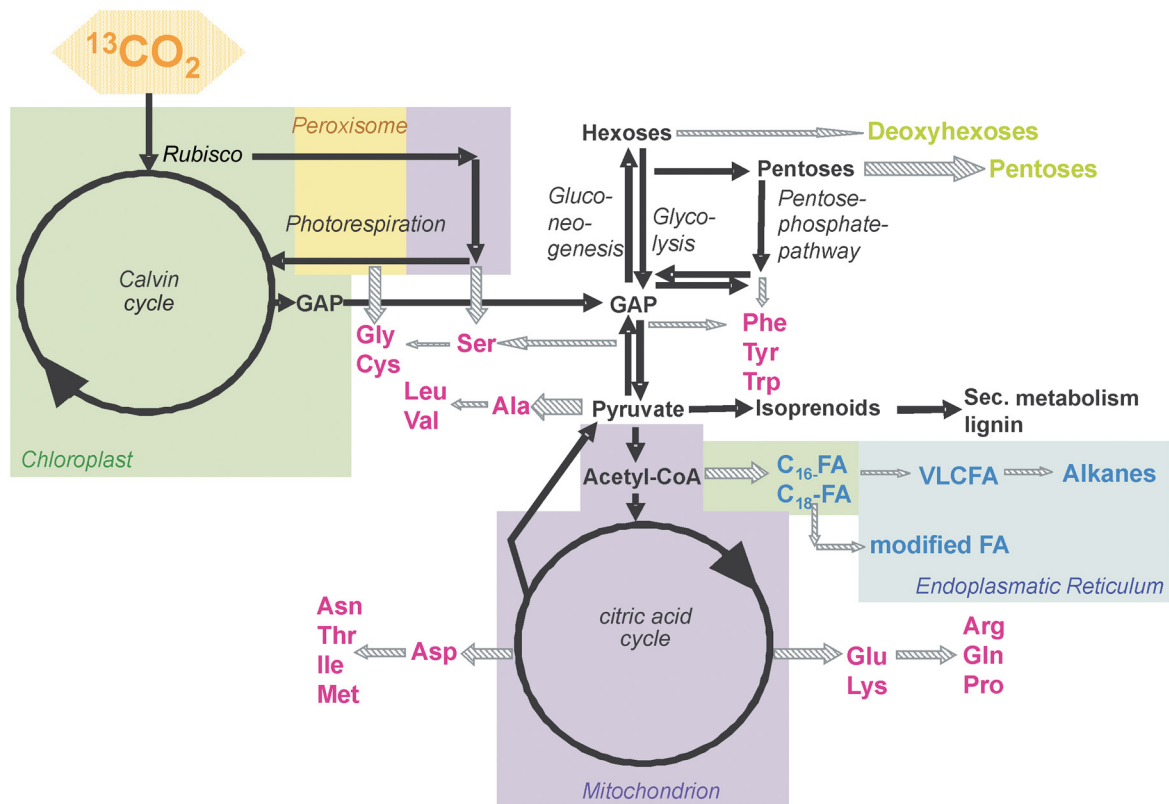


Figure 1. Simplified scheme of basic C fluxes in the needle after ^{13}C assimilation traced in this study. Boxes represent cell organelles. Processes out of all boxes take place in the cytosol. Diagonally hatched arrows indicate relative C flux towards the investigated compounds within the class of amino acids (central and lower part of the figure), hemicellulose-derived sugars (upper right part of the figure) and lipids (middle right part of the figure).

~9-year-old Norway spruce trees were selected, of which five were labelled with ^{13}C . The labelled trees had an average height of 315 ± 14 cm, a stem diameter at the base of 7.4 ± 0.3 cm and a needle mass of 2350 ± 250 g. The unlabelled trees served as $\delta^{13}\text{C}$ references for tracer uptake calculations. ^{13}C short-term pulse labelling was carried out on 2 May (three trees) and 3 May (two trees), respectively over a 6-h period from 10 am to 4 pm. The average air temperature during this sunny period was 19.6 ± 0.4 and 20.5 ± 0.4 °C, respectively.

^{13}C labelling

^{13}C pulse labelling was performed according to Glaser et al. (2012). In brief, the selected trees were exposed to a ^{13}C -enriched CO_2 atmosphere under transparent gas-tight plastic foil shapes. Bottles filled with 4 M H_2SO_4 were fixed at the stems at ~150 cm height. Then glass burettes containing the tracer solution, i.e., 11 g of $\text{Na}_2^{13}\text{CO}_3$ (99 at% ^{13}C , Cambridge Isotope Laboratories, Andover, MA, USA) dissolved in deionized water and fitted with adjustable stopcocks, were installed above the H_2SO_4 reservoirs. Small fans were placed in the middle of the treetops to distribute the produced $^{13}\text{CO}_2$ homogeneously. After covering the trees with the plastic shapes, the burette stopcocks were opened so that the tracer solution slowly dripped into the acid. In general, each tree was labelled with 33 g of

$\text{Na}_2^{13}\text{CO}_3$ tracer for 6 h. The tracer was applied in three equal portions every 2 h to improve the distribution of $^{13}\text{CO}_2$ within the labelling chamber and to avoid high CO_2 enrichment under the plastic cover.

Sampling and preparation of bulk plant material, WSOC and stOC

After 6 h of labelling, the cover was removed and the trees felled and cut into pieces. Immediately afterwards, representative mixed samples of the green needles and four samples per stem segment and branch type of each of the labelled as well as of the reference trees were frozen and freeze-dried. All samples were ground with a ball mill to a fine powder (Retsch M2009) to extract the needle compound classes. The remaining tree biomass was dried at 50 °C for 6 months using special heat lamps to better separate the different tree compartments (stem segments, different branch types and needles) and obtain precise dry weights, especially of the bigger stem segments.

Water-soluble organic C was extracted following Gessler et al. (2004). Fifty milligrams of freeze-dried needles were incubated in 1 ml of deionized water at 5 °C for 1 h. After heating to 100 °C, keeping constant temperature for 3 min and precipitation of proteins, the extracts were centrifuged for 5 min at 12,000 r.p.m. Prior to C quantification and further isotope analysis, supernatants

were filtered through glass fibre filters to remove non-dissolved particles, freeze-dried and reweighed. Non-hydrolysable structural organic C was determined after sequential extraction of the compound classes, i.e., total lipid extraction and strong acid hydrolysis with 6 M HCl for 10 h. Extractable compounds were removed by filtration and the residue was reweighed and freeze-dried for subsequent isotope analysis.

Extraction of the needle compound classes

Hydrolysis and purification of amino acids Free and protein-bound amino acids were extracted according to Amelung and Zhang (2001) with slight modifications. In brief, amino acids from each sample containing 10 mg total organic carbon (TOC) were gained by acid hydrolysis at 105 °C for 10 h. Subsequently, 35 µg of l-norvalin dissolved in 100 µl of 0.1 M HCl was added to the hydrolysates as first internal standard. After filtration through glass fibre filters (MN GF-6, Macherey-Nagel, Dueren, Germany), HCl was removed by rotation evaporation. Extracts were purified on Dowex 50 WX8 ion exchange resins (100–200 mesh, SERVA, Heidelberg, Germany) and the eluted amino acids were freeze-dried. Prior to derivatization, 35 µg of the second internal standard—trans-4-(aminomethyl) cyclohexane carboxylic acid—was added to each sample. For esterification, 500 µl of water-free 4 M HCl was used, and for acetylation, 150 µl dichloromethane (DCM) and 150 µl pentafluoropropionic acid anhydride were added.

Hydrolysis and purification of neutral sugars The hemicellulose sugars arabinose, xylose, rhamnose and fucose were extracted and purified following the procedure described by Amelung et al. (1996). Samples containing ~10 mg TOC were hydrolysed for 4 h at 105 °C after adding 100 µg of the first internal standard myo-inositol and 10 ml of 4 M trifluoroacetic acid (TFA). The hydrolysed samples were filtered with a glass fibre filter (MN GF-6, Macherey-Nagel) to remove the plant residues from the extracted monosaccharides and then dried using a rotary evaporator to completely eliminate the TFA. After redissolving in distilled water, samples were purified on a column system with an adsorption resin (XAD-7, SERVA) and a cation-exchange resin (Dowex 50 WX8, SERVA). The derivatization of the freeze-dried eluates was carried out using the methylboronic acid method described by van Dongen et al. (2001). In brief, first 100 µg of 3-O-methylglucose in pyridine as second internal standard was added to each sample and to an external standard series of the investigated monosaccharides. The sugars and standards were derivatized with 4.5 mg methylboronic acid in 450 µl water-free pyridine by heating to 60 °C for 1 h and thereafter immediately cooled down in a refrigerator to stop the chemical reaction. For measurement, samples were redissolved in 400 µl ethylacetate and transferred into vials.

Extraction of cellular and cuticular and of the epicuticular free wax lipids Freeze-dried spruce needles (1.1–3.0 g) were

weighed in extraction ferrules and submerged in DCM picograde for 1 min (Kreyling et al. 2012) to obtain the epicuticular wax lipids. After separation of the epicuticular wax lipids, the needles were dried and ground by a ball mill (Retsch M200) and extracted by standard Soxhlet extraction for 36 h using a solvent mixture of DCM/methanol (93 : 7; v : v) (Wiesenberg et al. 2010). Then, dried internal (mixture of cellular and cuticular lipids) as well as epicuticular lipid extracts were purified by an identical method: fatty acid and alkane fractions were sequentially separated using solid-phase extraction. Aliquots of both extracts were redissolved in DCM and transferred to KOH-coated silica gel columns. The neutral lipid fraction was eluted by rinsing the columns with DCM and the acid lipid fraction by using a solvent mixture of DCM/formic acid (99 : 1; v : v) (Wiesenberg et al. 2010). To separate alkanes from polycyclic aromatic compounds, ketones and alcohols, the neutral lipid fraction was dissolved in hexane, transferred to columns filled with activated silica gel (100 Å, Supelco, Sigma-Aldrich, Taufkirchen, Germany) and rinsed with hexane.

While for alkanes no further preparations were necessary, fatty acids were derivatized by methylation with boron trifluoride-methanol solution (BF₃, 10%, FLUKA, Sigma-Aldrich) for 15 min at 60 °C and subsequently separated from the derivatization reagent by liquid–liquid extraction with DCM after adding deionized water (Wiesenberg et al. 2010). After repeated extraction, the combined DCM phases were transferred to columns filled with sodium sulphate to remove the water and directly collected in autosampler vials. Prior to measurements, the deuterated internal standards D₃₉C₂₀ and D₅₀C₂₄ were added to each sample and to external standard series of the fatty acid and the alkane fractions.

Stabile isotope analyses

Bulk, WSOC and stOC measurements Solid samples were finely ground with a ball mill. Freeze-dried samples of the tree compartments and freeze-dried aliquots of the WSOC and stOC were weighed into tin capsules for isotope ratio mass spectrometry analysis. δ¹³C and total C were determined using a combination of an elemental analyser (EA, Carlo Erba NC 2500) and an isotope ratio mass spectrometer (Delta^{Plus}), which were connected via a ConFlo III interface (all instruments from Thermo Finnigan, Bremen, Germany). Helium (99.996% purity; Riessner, Lichtenfels, Germany) served as carrier gas. Calibration was carried out with certified standards: sucrose (IAEA-CH-6, IAEA, Vienna, Austria), polyethylene (IAEA-CH-7), glutamic acid (USG-41, IAEA) and acetanilide (Carlo Erba Instruments, Milan, Italy). Within a measurement sequence, all standards were measured repeatedly together with the samples.

Compound-specific isotope analysis Compound-specific isotope measurements of the needle-derived substance classes were carried out with a gas chromatograph-combustion-isotope ratio mass spectrometer (GC-C-IRMS) consisting of a Trace GC

2000 gas chromatograph coupled via a GC combustion III interface to a Delta^{Plus} isotope ratio mass spectrometer (all instruments from Thermo). Samples were injected into the gas chromatograph with a 10- μ l syringe (Hamilton, Switzerland) by an AS 2000 autosampler (Thermo Finnigan). Chromatography was performed by an Agilent J&W DB-5MS column (60 m \times 0.25 mm \times 0.25 μ m film thickness) with helium (99.996% purity; Riessner) as carrier gas.

The different compound classes were measured with individual temperature and injector programmes as follows: amino acid measurements were performed according to Sauheitl et al. (2009) and hemicellulose measurements according to Sauheitl et al. (2005). For fatty acids, a measurement programme for PLFA (Gunina et al. 2014) was slightly modified by decelerating the final ramp from 185 to 290 $^{\circ}$ C at a rate of 2.5 $^{\circ}$ C min⁻¹ to enable baseline separation of the very long-chain fatty acids (VLCFAs, 20:0–30:0). Alkane measurements were performed according to Zech and Glaser (2008). To quantify various compounds, external standard dilution series were prepared in five concentrations covering the sample range, derivatized and measured identically to the samples. The quantification was calibrated by the external standard line according to Gunina et al. (2014). $\delta^{13}\text{C}$ values were calibrated online by measuring several CO_2 reference gas pulses (99.7% purity; Riessner) and corrected for derivatization C and amount dependency based on the external standards as described by Glaser and Amelung (2002). Therefore, $\delta^{13}\text{C}$ values of all individual external standard compounds were measured as underivatized compounds by EA-IRMS with the instrumental set-up used for the bulk measurement mentioned above.

Calculations

For all the following calculations, the $\delta^{13}\text{C}$ values obtained by the isotope measurements were converted to at% ^{13}C according to Craig (1953). Based on the assumption that the trees took up $^{13}\text{CO}_2$ of known isotopic composition (99 at% $^{13}\text{C}_t$), the ^{13}C uptake into the different tree compartments was calculated according to a two end-member mixing model described by Gearing (1991) as

$$C_m \times \text{at\% } ^{13}\text{C}_m = C_b \times \text{at\% } ^{13}\text{C}_b + C_t \times \text{at\% } ^{13}\text{C}_t \quad (1)$$

$$C_m = C_b + C_t \quad (2)$$

C_m , C_b and C_t are the amount of C in the labelled sample (m), background sample (b) and taken up amount of C of the applied tracer (t) (mol g⁻¹), respectively, and at% $^{13}\text{C}_m$, at% $^{13}\text{C}_b$ and at% $^{13}\text{C}_t$ = abundance of the isotope ^{13}C in the mixture, background and tracer (%). Solving Eq. (1) to C_t after substitution of C_b by Eq. (2) gives the amount of tracer-C taken up into a sample.

The relative uptake into individual tree compartments was calculated by the uptake of tracer-C as the portion of the applied

tracer (Eq. (3)). The applied tracer is the amount of ^{13}C carbonate, which was converted under the foil shapes quantitatively to $^{13}\text{CO}_2$. $^{13}\text{C}_{\text{up}}$ of the individual tree compartments represents the portion of tracer-C taken up from the applied tracer-C (C_{app}) in per cent:

$$^{13}\text{C}_{\text{up}} = \frac{C_t}{C_{\text{app}}} \times 100\% \quad (3)$$

^{13}C allocation into tree compartments was calculated based on the portion of ^{13}C taken up into an individual tree compartment to the total amount of ^{13}C taken up into the entire above-ground tree biomass. Similarly, allocation into individual compound classes was calculated by dividing the amount of tracer taken up into an individual needle compound class by the amount of total tracer-C taken up by all measured compound classes. ^{13}C allocation between individual compounds of a certain compound class was calculated by dividing the allocation of C taken up into an individual compound by the sum of the uptake C_t of all compounds measured for this class. Thus, in each case, the allocation describes the relative distribution of the assimilated C between tree compartments, leaf compound classes or individual compounds.

Additionally, a parameter describing the percentage of a certain C pool de novo synthesized from the assimilated ^{13}C was calculated and named ^{13}C enrichment ($^{13}\text{C}_{\text{enrich}}$) throughout this study (Eq. (4)).

$$^{13}\text{C}_{\text{enrich}} = \frac{C_t}{C_c} \times 100 \quad (4)$$

C_t is the amount of ^{13}C and C_c the C pool size of the individual tree compartments, compound classes and compounds, both in mol.

Statistical analysis

Data were presented as mean values of at least three replicates and standard error (SE). As our data were not normally distributed, Kruskal–Wallis analysis of variance was conducted to test for significant differences using the Statistica 7.0 package (version 7.0, StatSoft Inc., Tulsa, OK, USA). Whenever a significant difference was detected, multiple comparisons of mean rank differences were analysed using the method of Conover (1980) as post hoc test at a 0.05 significance level.

Results

^{13}C uptake and distribution within tree compartments

After 6 h of pulse labelling, 75.7% of the applied tracer- $^{13}\text{CO}_2$, i.e., the added carbonate-derived $^{13}\text{CO}_2$, was detected in the above-ground tree biomass. Be aware that this proportion is relative to net assimilation, i.e., may be even higher if a significant amount of C was first assimilated and then respired in the course of 6 h. Most (85.5%) of this assimilated ^{13}C was localized in the needles, while 12.9% were allocated to various

branch types and 1.6% into the stem (Figure 2a). This 1.6% stem ^{13}C showed a clear allocation pattern with height: relative stem ^{13}C allocation increased significantly from the top (4.9%) to a stem height of 50 cm (30.5%), while in the bottom stem segment (0–50 cm) farthest away from the needles, only ~4.9% incorporated ^{13}C was detected (Figure 2b).

The allocation describes the fate of tracer- ^{13}C . In contrast, the ^{13}C enrichment demonstrates the relative contribution of assimilated ^{13}C for the respective C pool. Considering not entire stem biomass but assuming ^{13}C enrichment only in the active stem tissue, i.e., the outer 4 mm (Franceschi et al. 2000, Gall et al. 2002), the ^{13}C enrichment pattern follows the allocation pattern (Figure 2b).

Comparing over all tree compartments (needles, various branches, stem), the ^{13}C enrichment was highest for the needles, where 0.21% of the needle C was comprised of recently assimilated tracer-C. The ^{13}C enrichment increased with decreasing branch size and thus a decreasing C pool of the branch (Figure 2a; Table 1).

Allocation and enrichment of ^{13}C in needle compound classes

The contents of the investigated compound classes in the needles covered a wide range: the largest compound class we

quantified by compound-specific isotope analysis was the amino acids (96 mg g $^{-1}$), whereas the needle-derived alkanes amounted to only 0.017 mg g $^{-1}$ (Figure 3a). Generally, needles contained, besides stOC, higher contents of water-soluble compound classes such as WSOC, hemicellulose-derived sugars and amino acids than of fatty acids and alkanes. Comparing cellular and cuticular with the epicuticular layer, ~10 times less fatty acids but two times more alkanes were detected in the epicuticular layer (Figure 3a).

In total, 52.9% of the ^{13}C incorporated in the whole needle biomass during the 6-h labelling period was recovered in the WSOC, stOC and the four compound classes (Table 2). Most of the assimilated ^{13}C was allocated to WSOC (44.1%) and stOC (33.9%), followed by amino acids (20.6%) > hemicellulose sugars (1.0%), compared with quantitatively small lipid classes such as fatty acids and alkanes (0.3 and 0.0002% ^{13}C , respectively) (Figure 3b). Some 47.1% of the bulk needle ^{13}C could not be attributed to one of the investigated pools and has to be attributed to pools that got lost or were not considered (ribonucleotides, several lipid classes like aromatic compounds, terpenes, etc.) in the described sequential extraction procedure. While a similar allocation of ^{13}C was observed for the cellular and cuticular alkanes on the one hand and epicuticular alkanes on the other, the allocation of ^{13}C into the fatty acids differed significantly by a magnitude of

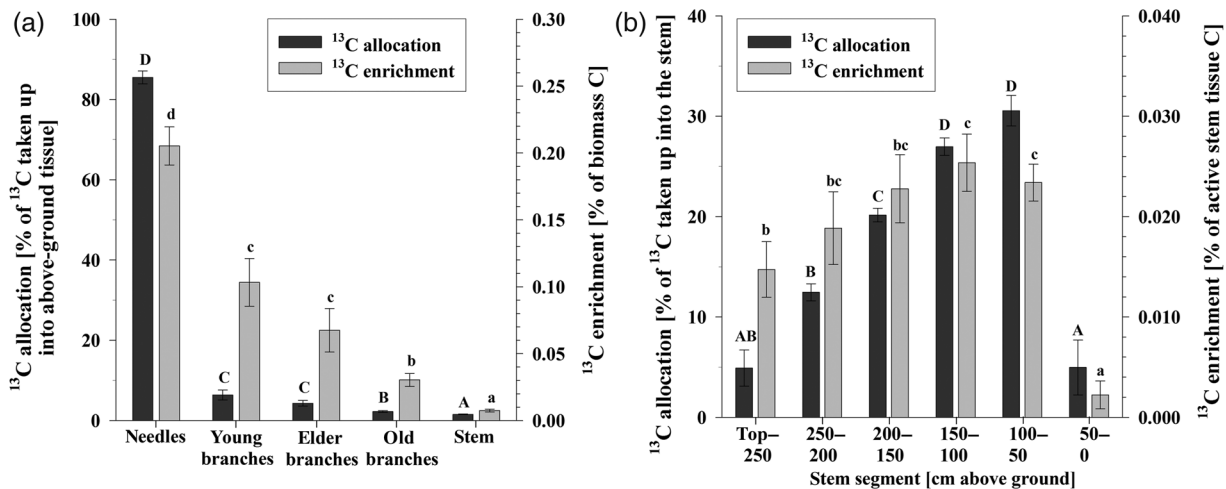


Figure 2. (a) Allocation of ^{13}C (% of ^{13}C recovery in above-ground tissue) taken up by the tree compartments (dark grey bars) and ^{13}C enrichment (% of compartment biomass C) of individual tree compartments (light grey bars). (b) Allocation of ^{13}C into stem segments (% of ^{13}C recovered in stem) and ^{13}C enrichment (% of active stem tissue C). Letters indicate significant differences between tree compartments (a) and stem segments (b) ($P < 0.05$), with capital letters representing allocation and lower case letters representing ^{13}C enrichment data. Given are mean values of at least five replicates \pm SE.

Table 1. C pool sizes of the different tree compartments and stem segments. Data show mean \pm SE ($n = 5$).

	Tree compartment				Stem	Stem segment (cm above ground)					
	Needles	Young branches	Elder branches	Old branches		Top-250	250-200	200-150	150-100	100-50	50-0
C pool (g C per compartment or stem segment)	1176.4 \pm 122.5	194.8 \pm 15.8	227.5 \pm 35.3	220.3 \pm 24.0	584.7 \pm 15.7	40.8 \pm 8.3	70.3 \pm 4.1	89.1 \pm 6.9	102.5 \pm 6.0	120.2 \pm 5.2	161.7 \pm 8.4

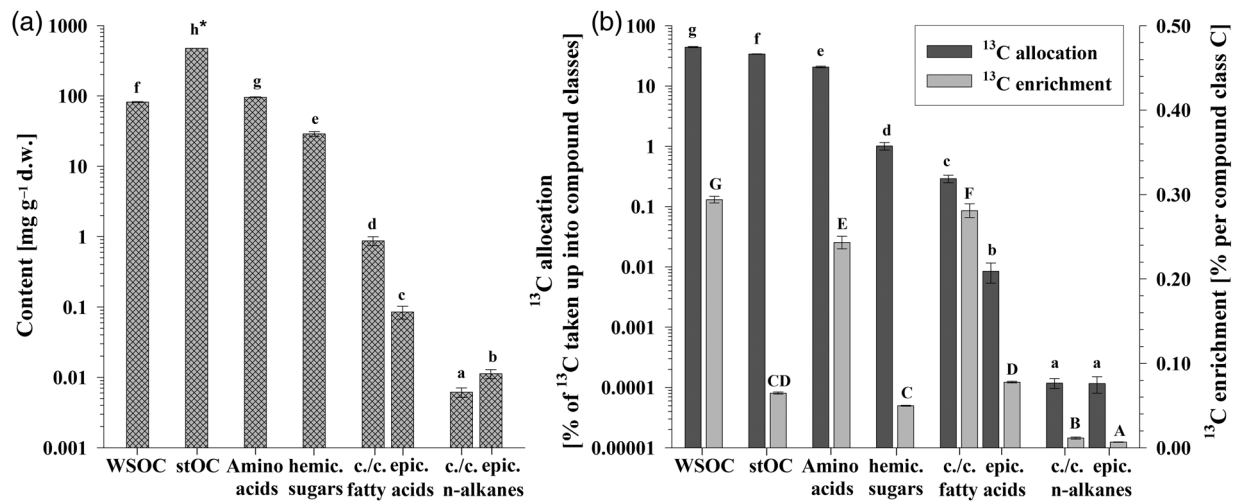


Figure 3. (a) Contents of individual compound classes in spruce needles (* shows value adapted from Springer and Lehner 1952). (b) Allocation of ¹³C (in % of ¹³C recovered in all compound classes) in the compound classes (dark grey bars) and ¹³C enrichment per total C of each compound class (in % of compound class C) (light grey bars). Capital and lower case letters show significant differences between compounds ($P < 0.05$). WSOC, stOC, hemic., c./c. and epic. are abbreviations for water-soluble organic C, non-hydrolysable structural organic C, hemicellulose, cellular/cuticular and epicuticular, respectively. Means of at least three replicates \pm SE are presented.

Table 2. Absolute ¹³C recovery in the compound classes (in % of total needle-assimilated ¹³C). WSOC, stOC, c./c. and epic. are abbreviations for water-soluble organic C, non-hydrolysable structural organic C, cellular/cuticular and epicuticular, respectively. Additionally, ¹⁵N recovery in the water-soluble organic fraction and the non-hydrolysable structural organic fraction is presented (in % of total needle-assimilated ¹⁵N). Data show mean \pm SE ($n = 3$).

	Compound class							
	WSOC	stOC	Amino acids	Hemicellulose sugars	c./c. fatty acids	epic. fatty acids	c./c. alkanes	epic. alkanes
¹³ C recovery (% of total ¹³ C taken up into the needle)	23.6 \pm 0.5	18.2 \pm 0.3	10.3 \pm 0.4	0.6 \pm 0.05	0.18 \pm 0.03	0.005 \pm 0.001	0.00007 \pm 0.00001	0.00006 \pm 0.00001
¹⁵ N recovery (% of total ¹⁵ N taken up into the needle)	Water-soluble organic fraction 14.0 \pm 0.7	Structural organic fraction 27.4 \pm 0.8						

36 between the cellular and cuticular pool (0.29%) and the epicuticular layer (0.008%; Figure 3b).

The ¹³C enrichment per C pool differed significantly between the compound classes (Figure 3b). The highest ¹³C enrichment was detected in the WSOC, where 0.3% of the C pool was comprised by assimilated ¹³C. In contrast, stOC and hydrolysable, structural hemicelluloses had rather low enrichment (<0.1%).

The disproportionately high ¹³C enrichment of the cellular and cuticular fatty acids compared with the ¹³C allocation into this compound class demonstrates the active de novo synthesis and fast turnover of this compound class. In contrast, the alkanes showed the lowest portion of ¹³C enrichment, reflecting slow biosynthesis and turnover of this pool. For both lipid compound classes, the ¹³C enrichment was significantly lower in the epicuticular layer than in the cellular and cuticular pool (four and two times for fatty acids and alkanes, respectively, Figure 3b).

Allocation and enrichment of ¹³C in individual amino acids

The content of amino acids differed within a magnitude of 16: methionine had the lowest and alanine the highest contents (1.0 and 15.9 mg g⁻¹, respectively, Figure 4a). Most ¹³C was allocated into the highly abundant amino acids alanine, glycine and glutamine. Together with serine, ~73% of the ¹³C was allocated into these four amino acids (Figure 4b). In contrast, comparatively little ¹³C (~16.8%) within the amino acid pool was allocated to leucine, valine, proline and phenylalanine, which occurred in relatively high quantities, too (Figure 4a). Consistent with its low abundance, methionine had the lowest portion of ¹³C allocation (0.7%).

Not only tracer-¹³C allocation but also the ¹³C enrichment was highest for serine, glycine and alanine with 0.72, 0.53 and 0.5% of the amino acid C, respectively (Figure 4b). Compared with the low allocation of the assimilated tracer-¹³C into methionine, the ¹³C enrichment was relatively high, i.e., assimilated ¹³C comprised 0.2% of the methionine pool. In contrast, the ¹³C enrichment of

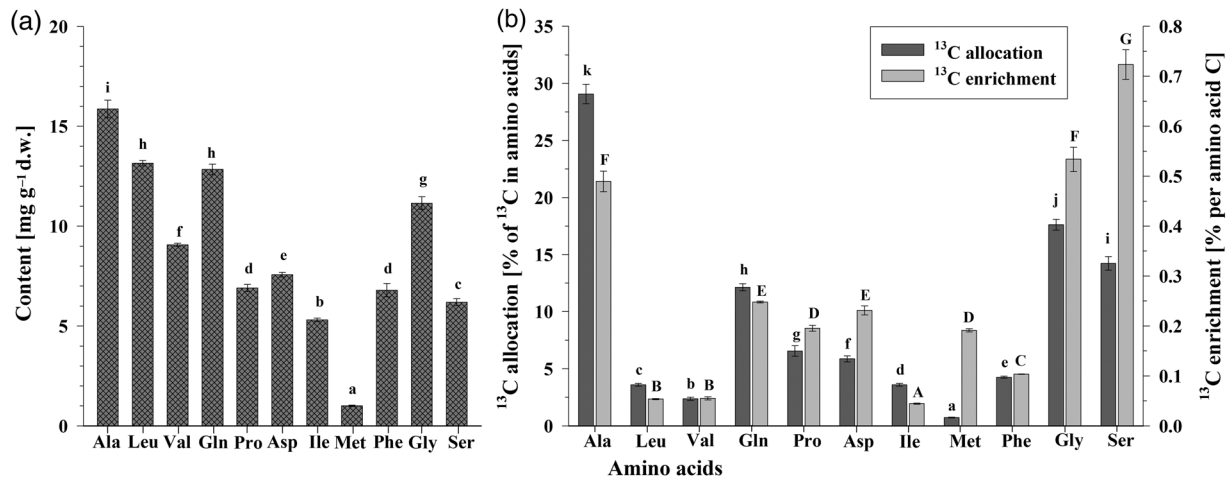


Figure 4. (a) Amino acid contents in spruce needles. d.w., dry weight. (b) Allocation of ¹³C into individual amino acids (% of ¹³C recovered in amino acids) (dark grey bars) and ¹³C enrichment of the individual amino acid pools (% ¹³C per amino acid C) (light grey bars). Results for the 11 proteinogenic amino acids are represented: Ala (alanine), Leu (leucine), Val (valine), Gln (glutamine), Pro (proline), Asp (asparagine), Ile (isoleucine), Met (methionine), Phe (phenylalanine), Gly (glycine) and Ser (serine). Capital and lower case letters show significant differences between compounds ($P < 0.05$). Means of at least three replicates \pm SE are presented.

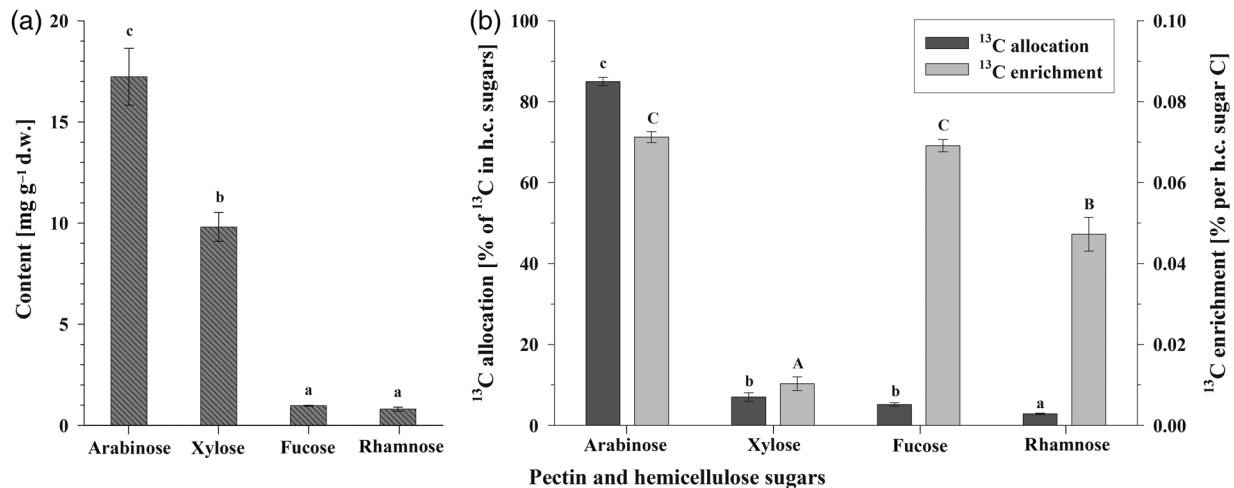


Figure 5. (a) Contents of pectin and hemicellulose sugars in spruce needles. d.w., dry weight. (b) Allocation of ¹³C into the individual hemicellulose (h.c.) sugar monomers (% of ¹³C recovered in h.c. sugars) (dark grey bars) and ¹³C enrichment of the individual h.c. sugar pools (% ¹³C per h.c. sugar C) (light grey bars). Capital and lower case letters show significant differences between compounds ($P < 0.05$). Means of at least three replicates \pm SE are presented.

isoleucine, leucine, valine and phenylalanine was low, comprising <0.1% of the respective amino acid C (Figure 4b).

Allocation and enrichment of ¹³C in individual pectin- and hemicellulose-derived sugars

Pentoses dominated the hemicellulose fraction in needles, with arabinose reaching twice the content of xylose (17.2 and 9.8 mg g⁻¹) and ~20 and 10 times the content of the deoxyhexoses fucose and rhamnose with an average of 0.9 mg g⁻¹ (Figure 5a).

The ¹³C allocation into the individual sugars followed mostly the order of their abundance (Figure 5b): ~85% of hemicellulose ¹³C was allocated into arabinose and only 2.9% into rhamnose. Only a low ¹³C allocation, however, was found for xylose (~7% of

the total ¹³C in hemicelluloses) even though it was the second most common sugar. Consequently, the ¹³C enrichment of xylose was also lowest, not exceeding 0.01% of the xylose-C pool (Figure 5b). In contrast, the small pools of deoxyhexoses showed a high ¹³C enrichment exceeding 0.05% of their C pool size; this was in the same range as the ¹³C enrichment of the most abundant hemicellulose-derived sugar arabinose.

Allocation and enrichment of ¹³C in individual fatty acids

Within the cellular and cuticular fatty acids, a clear even-over-odd predominance is evident for the short-chain (14:0–15:0) and mid-chain (16:0–18:0) fatty acids, whereas this pattern is less pronounced for the VLCFAs (Figure 6a). The two biosynthetic precursor fatty acids, palmitic acid (16:0) and oleic acid (18:1),

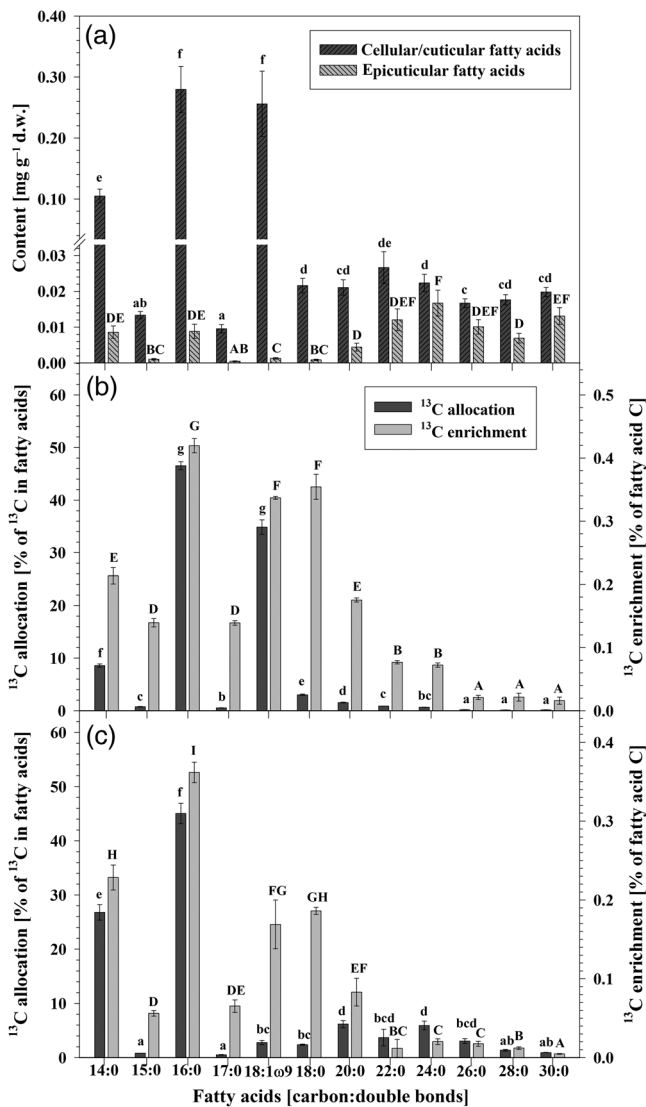


Figure 6. (a) Contents of cellular and cuticular (grey bars) and epicuticular fatty acids (dark grey bars) in spruce needles. d.w., dry weight. Allocation of ^{13}C into individual cellular and cuticular (b) and into epicuticular (c) fatty acids (% of ^{13}C recovered in fatty acids) (dark grey bars). ^{13}C enrichment of individual cellular and cuticular (b) and in epicuticular (c) fatty acids (% ^{13}C per fatty acid C) (light grey bars). Capital and lower case letters show significant differences between compounds ($P < 0.05$), and ω indicates position of double bond. Means of at least three replicates \pm SE are presented.

were the most abundant fatty acids. Very long-chain fatty acids occurred in significantly lower amounts than short- and mid-chain saturated fatty acids.

Most (~81%) of the assimilated ^{13}C of all fatty acids were present in palmitic and oleic acids (Figure 6b). Considerably less ^{13}C was allocated in all other fatty acids, decreasing continuously with increasing chain length (Figure 6b). Besides palmitic and oleic acids, a high percentage of stearic acid C (18:0) was enriched by assimilated ^{13}C , reflecting the role of stearic acid as intermediate between palmitic and oleic acids and thus having a similar ^{13}C dynamic.

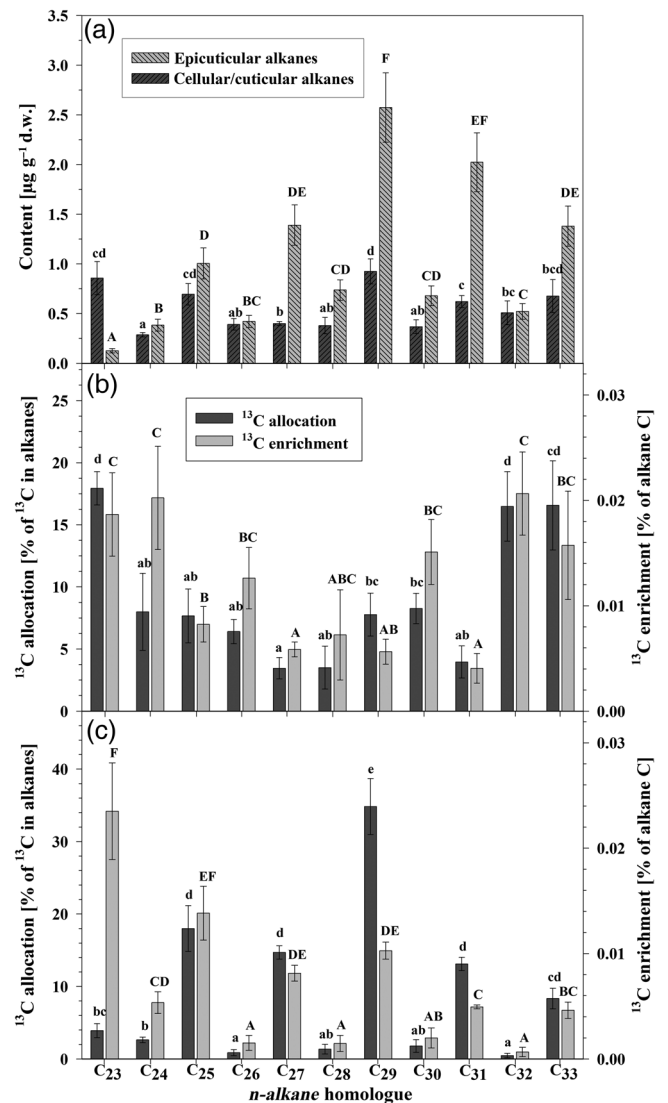


Figure 7. (a) Contents of cellular and cuticular (grey bars) and epicuticular alkanes (dark grey bars) in spruce needles. d.w., dry weight. Allocation of ^{13}C into individual cellular and cuticular (b) and into epicuticular (c) alkanes (% of ^{13}C recovered in alkanes) (dark grey bars). ^{13}C enrichment of individual cellular and cuticular (b) and in epicuticular (c) alkanes (% ^{13}C per alkane C) (light grey bars). Capital and lower case letters show significant differences between compounds ($P < 0.05$). Means of at least three replicates \pm SE are presented.

In the epicuticular layer, VLCFAs constitute the dominant group of the investigated fatty acids (Figure 6a), except for myristic acid (14:0) and palmitic acid (16:0), which were in the range of the VLCFAs.

About 72% of the ^{13}C detected in the epicuticular fatty acids was allocated to palmitic and myristic acids (Figure 6c). Within VLCFAs, ^{13}C allocation was highest in lignoceric acid (24:0) and decreased with increasing chain length. Despite the high abundance of VLCFAs in the epicuticular layer, the ^{13}C allocation into the epicuticular VLCFAs was 10 times lower compared with palmitic and myristic acids.

Similar to the cell interior, the highest ^{13}C enrichment per amount of C was detected in palmitic, myristic, stearic and oleic acids, indicating an exchange between the cellular and cuticular and the epicuticular pool already within the 6-h labelling (Figure 6c).

Allocation and enrichment of ^{13}C in individual alkanes

A tendency towards an odd-over-even predominance was detected in the cellular and cuticular alkanes, which got lost with increasing chain length (Figure 7a). Even within the short-chain alkanes, however, this odd-over-even predominance was not reflected in the allocation of assimilated ^{13}C : ^{13}C was similarly allocated between odd- and even-numbered alkanes with chain lengths between 24 and 31 C atoms; only C_{23} , C_{32} and C_{33} alkanes received significantly higher amounts of ^{13}C (Figure 7b).

The lowest ^{13}C enrichment within the cellular and cuticular alkanes was detected in the odd-numbered alkanes C_{27} , C_{29} and C_{31} (Figure 7b). Interestingly, these are the most abundant alkanes in the epicuticular alkane pool but not in the cellular and cuticular pool.

The contents of the individual alkanes in the epicuticular waxes differed significantly and showed a clear odd-over-even predominance, with the highest contents for C_{27} , C_{29} and C_{31} (Figure 7a). Within both odd- and even-numbered alkanes, alkanes with the shortest chain lengths had lowest contents in each case.

In line with the predominance of the odd-numbered alkanes, the ^{13}C allocation within the epicuticular alkanes was 13 times higher in odd- versus even-numbered alkanes and peaked in C_{29} (Figure 7c). The pattern of ^{13}C allocation (Figure 7b) resembled the pattern of its abundance (Figure 7a). This demonstrates that those alkanes with high contents in the epicuticular waxes were also highly enriched with freshly assimilated C.

Discussion

Uptake and allocation of assimilated C into tree sink tissues

About 84% of the assimilated C remained in the needles after the ^{13}C labelling (Figure 2a), indicating investment for growth 15 days after bud burst. The metabolic C demand in spring is exceptionally high in the tree canopy for many physiological processes such as bud break, shoot sprouting and needle growth (Hansen and Beck 1994). This high C demand can be covered by stored reserves (mainly starch) or assimilated C (Ericsson 1978). Studies on other conifers such as Scots pine also showed that 1-year-old as well as current year needles and shoots were the main sinks of photosynthates during and after bud break (Lippu 1994, Pumpanen et al. 2009).

A smaller portion (16%) of assimilated ^{13}C was allocated to branches and stem 6 h after start of labelling (Figure 2a), suggesting fast translocation of assimilates with phloem sap. Small

portions of recently assimilated C in the twigs have also been associated with photosynthetic activity of the twig cortex rather than assimilate export by the needles because various tree species show detectable stem photosynthesis in young green twigs and stems (Damesin 2003). In this study, however, the small but detectable proportion of ^{13}C allocated to the basic stem segment clearly indicates phloem transport of the assimilated C (Figure 2b) because this segment had no branches and was excluded from fumigation with $^{13}\text{CO}_2$. The observed transport distance after 6 h is in agreement with transport rates for coniferous trees (Brandes et al. 2006, Dannoura et al. 2011). The high allocation of assimilated ^{13}C into the WSOC of the needles (Figure 3b) also confirms that a significant portion of the assimilated C is used for the synthesis of transportable molecules and not for immediate incorporation into polymeric cellular tissue (i.e., the stOC and hemicellulose pool). The pronounced high allocation of recently assimilated C to needles could also partly be due to the relatively short duration between labelling and sampling. In summary, most of the assimilated C remained in the needles, while only a minor portion was transported towards stems and possibly to roots. This may be used for continued root growth, which in conifers already starts before bud break (Konôpka et al. 2005).

Incorporation and allocation of ^{13}C into individual needle compound classes

Six hours after ^{13}C labelling, ~52.9% of the total incorporated ^{13}C of the needle was recovered in the analysed compound classes. The remaining 47.1% could not be assigned to specific compounds and were presumably incorporated into the not considered compound classes like ribonucleotides, terpenes and aromatic lipids. Similar allocation patterns of ^{13}C between the investigated compound classes and their abundance (Figure 3b) indicate de novo synthesis of all relevant compound classes required for needle tissue growth.

In contrast, the incorporation of ^{13}C into the compound classes is inconsistent with the pool size of the compound classes: hemicellulose sugars and stOC show a rather low enrichment of their rather large pools by newly assimilated ^{13}C , even though a high amount of ^{13}C was allocated into these pools (Figure 3b). This does not necessarily indicate a lower de novo synthesis of these compound classes. It can also be attributed to the allocation of old, stored C into the cell walls of young, growing needles because the cell wall formation of sprouting needles is supported by the photosynthesis products of the previous year's needles (Hansen and Beck 1994). Similarly, C allocation from stored C pools is likely to occur and may dilute the recently assimilated C in the Norway spruce hemicellulose and stOC fraction (Figure 3b).

The high ^{13}C allocation into amino acids demonstrates that amino acids are a fast-reacting pool with rapid turnover in growing plant tissue. High incorporation of ^{15}N into the water-soluble

organic fraction of the needles (6 h after stem labelling, Table 2) also confirms the fast *de novo* synthesis of amino acids, which are the major N transport compounds in plants (Herschbach et al. 2012).

Even though the absolute amount of ^{13}C allocated into fatty acids is lower than into amino acids, the smaller pool size of fatty acids causes a similar enrichment of the fatty acid pool by recently assimilated C. This is common because lipids serve many functions within plant cells, including C storage or structural compounds of membranes and wax layers. Furthermore, the cellular fatty acids, especially 16:0 and 18:0, are the precursors of most lipid compounds in plant tissue (Kolattukudy 1970, Harwood and Russell 1984, Samuels et al. 2008).

The recovery of significant ^{13}C amounts in the epicuticular fatty acids and alkanes clearly demonstrates that biosynthesis and transport of fatty acids from their biosynthetic origin inside the cell towards the epicuticular layer is a fast process, taking <6 h (Samuels et al. 2008, Hurlock et al. 2014). The unexpectedly higher enrichment of the epicuticular fatty acids compared with the hemicellulose-derived sugars by ^{13}C can have several reasons: (i) turnover of epicuticular fatty acids is higher than turnover of cell wall hemicelluloses because of rapid *de novo* synthesis of cuticles of growing needles; (ii) regeneration of damaged wax layers of older needles is a fast process mainly involving recently assimilated C; and/or (iii) hemicellulose biosynthesis uses old, stored C as a C source.

Our data show that the use of freshly assimilated C plays a considerable role in fuelling the intensive metabolic demand of needle growth after bud break, but with clear differences in its allocation to different metabolite classes. Nevertheless, we were able to trace recently assimilated C in quantifiable amounts in each compound class, which is crucial for cell maintenance and growth. Consequently, the C allocation pattern we found can be used to trace the individual pathways of C metabolism in growing needle tissue.

Tracing major metabolic pathways by ^{13}C allocation into monosaccharides and amino acids

Monosaccharides and amino acids are monomeric compounds closely associated with the basic C metabolism of plants, i.e., photosynthesis and glycolysis (Heldt and Piechulla 2008) (Figure 1). Therefore, C allocation into these compounds can be used to specifically trace individual metabolic pathways at a certain stage of plant tissue development. While carbohydrates are direct products of photosynthesis, amino acids branch off all central glycolysis intermediates (Figure 1). Thus, metabolite tracing with compound-specific ^{13}C analyses of amino acids enables tracing C allocation within the basic metabolic network (You et al. 2012).

Extracting monosaccharides from bulk needle tissue by our method results in a co-extraction of free and hemicellulose-derived monosaccharides. Comparing our results with metabolome analysis

of free monosaccharides in needles of Norway spruce (Riikonen et al. 2012) and other conifers (Jansen et al. 2014) showed no dominance of arabinose, which is the dominant monosaccharide in our samples. In contrast, arabinose is the most abundant sugar in pectin and hemicelluloses of white spruce (Renault and Zwiazek 1997) and has further higher abundance than xylose in hemicelluloses of growing Norway spruce needles (Schädel et al. 2009). This hemicellulose-derived sugar pattern resembles strongly the pattern we observed in our hydrolysable sugar fraction and thus indicates that the monosaccharides in this study are indeed mainly hemicellulose derived.

Arabinose was not only the major compound but was also intensively synthesized *de novo* after bud break. This high *de novo* synthesis can be attributed to hemicellulose side-branch formation as well as to the biosynthesis of arabinogalactan proteins (AGPs), which contained ~30 mol% arabinose and up to 3 mol% fucose (Gaspar et al. 2001). Previous studies reported that hemicelluloses such as (arabino)glucuronoxylans, glucomannans and xyloglucans are the predominant types in primary and secondary cell walls of coniferous softwood (Timell 1967, Ebringerová 2005). This suggests a dominance of xylose as the main backbone monomer of the xylans. Incorporation of ^{13}C into xylose was significantly lower than into the monosaccharides of the side chains (arabinose, fucose and rhamnose) (Figure 5b). This indicates a higher formation or turnover of the hemicellulose side chains compared with the backbone. Moreover, AGPs may also be synthesized *de novo* in significant amounts, as they play crucial roles in plant development for embryogenesis, cell-cell interactions and cell proliferation (Burget et al. 2003). The high portions of ^{13}C incorporated into arabinose as well as into fucose (Figure 5b) indicate a fast formation of AGPs to facilitate needle growth and cell wall development, especially after bud break.

The highest ^{13}C portions were allocated into alanine, glycine and serine (Figure 4b), which suggests a fast formation of these amino acids. Interestingly, glycine and serine can be synthesized during photorespiration, in which phosphoglycolate formed by the oxygenase reaction of rubisco is recycled (Moroney et al. 2013). In an intermediate step, the amino group either of alanine or glutamate is transferred to glyoxylate, producing glycine, which is further converted to serine (Figure 1). The released ammonia of the latter reaction is then re-assimilated by glutamine (Moroney et al. 2013). The high content and ^{13}C incorporated into glutamine in this study underlines the importance of this pathway in this labelling experiment (Figure 4a and b). An increased oxygenase activity of rubisco during the labelling potentially reflects not only the young age of the foliage but also an increasing temperature and decreasing CO_2 to O_2 ratio under the plastic shape (Moroney et al. 2013).

In contrast, alanine was probably not produced during photosynthesis but is closely linked to the general C metabolizing pathway of glycolysis (Figure 1). As alanine is the aminated

form of pyruvate, one of the central C intermediates in metabolism, the fast formation of ^{13}C alanine indicates a rapid cycling of assimilated C through the basic C distributing pathways branching off from glycolysis. This is indicative for plant growth, where the fast formation of various precursor compounds is essential for biomass production. However, pyruvate is also a precursor for isoprenoids and thus for secondary metabolite biosynthesis (Priault et al. 2009). This pathway is known to be important for terpene synthesis in conifer needles (Ghirardo et al. 2010). Those authors even reported that 33% of emitted volatile monoterpene C is replaced by assimilated ^{13}C in *P. abies* needles 5 h after labelling. Thus, high ^{13}C enrichment in alanine may also point to a fast and highly active secondary metabolism.

A comparatively small ^{13}C portion was allocated to phenylalanine (Figure 4b). Nonetheless, considering the rather complex biosynthetic pathway of aromatic amino acids, the portion of incorporated ^{13}C is rather high. Phenylalanine acts not only as a proteinogenic amino acid but is also an important precursor of lignin biosynthesis as well as a precursor of secondary metabolism (Vogt 2010). The necessity for cell wall formation for needle growth, however, also suggests a high demand of phenylalanine for the formation of lignin monomers. Definitively distinguishing the fate of phenylalanine ^{13}C will require compound-specific analysis of volatile secondary metabolites as well as of lignin monomers.

The least abundant amino acid, methionine, shows interestingly high ^{13}C enrichment, i.e., >0.2% of the methionine pool was enriched by freshly assimilated C within 6 h (Figure 4b). This demonstrates that presumably a large portion of the cellular methionine is not bound in slow-cycling proteins, but rather has a precursor or intermediate function. Methionine is known to play an important role in C-1 metabolism, i.e., for methylation reactions such as methylation of DNA, formation of polyamines, vitamins, cofactors, osmoprotectants and hormones (Wirtz and Droux 2005). Its high turnover rate in the spruce needles compared with other amino acids (Figure 4b, see also Brückner and Westhauser 2003) can be attributed to the high methionine demand in these biosynthetic pathways, required for biomass production during intensive needle growth.

Lipid metabolism and export in growing needles

The most abundant fatty acids of the present study—palmitic acid (16:0), oleic acid (18:1) and stearic acid (18:0)—are the central precursors for all acetyl-CoA-derived lipids (Samuels et al. 2008) (Figure 6a). Their formation by the fatty acid synthase complex occurs in the plastids of all plant cells and is not restricted to specific tissues or organs (Li-Beisson et al. 2013). High contents of palmitic and oleic acids could reflect the degradation of the storage lipids triacylglycerols (Li-Beisson et al. 2013). Nonetheless, the high incorporation of freshly assimilated ^{13}C into palmitic and oleic acids we observed provides no indication for high mobilization of stored C. Instead, our study showed intensive de novo

synthesis of fatty acids (Figure 6b), confirming previous studies (Bao et al. 2000, Gao et al. 2012). Forty percentage of these de novo formed fatty acids are reported to remain in the plastids to form intracellular membranes, while 60% are transported to the endoplasmatic reticulum (ER) for further modifications such as elongation, desaturation or hydroxylation. Here, they contribute to intracellular membrane formation or become exported to the cuticle (Li-Beisson et al. 2013).

The present study reported highest ^{13}C allocation into the cellular and cuticular palmitic, stearic and oleic acids (Figure 6b). Besides their role as precursors for all other fatty acids, they are also present in diacylglycerols, which apparently accumulate in current-year needles of Scots pine (*Pinus sylvestris* L.) (Fischer and Höll 1991). This compound class is responsible for the formation of thylakoid membranes, i.e., the photosynthetic membranes of chloroplasts (Li-Beisson et al. 2013). The development of new photosynthetic membranes in growing needle tissue (Hansen et al. 1996) probably accounts for the high ^{13}C allocation into these fatty acids. This is supported by the high ^{13}C enrichment of serine (Figure 4b), a precursor of sphingolipids, which have key functions in intracellular membranes (Markham et al. 2011).

Incorporation of ^{13}C into VLCFAs was generally low and decreased continuously with increasing chain length (Figure 6b). This can indicate two things. Either their biosynthesis by elongation of palmitic, stearic and oleic acids in the ER by the fatty acid elongases is a rather slow process (>6 h) or their demand in the cuticle was rather low. Very long-chain fatty acids represent a major constituent of the epicuticular waxes in Norway spruce needles (Prügel and Lognay 1996). Nevertheless, a traceable allocation of ^{13}C into the VLCFAs of the epicuticular layer (Figure 6c) of this species demonstrates that biosynthesis of precursors, transport to ER, elongation and export from the ER to the epicuticular layer can take place even within 6 h (Gao et al. 2012). The higher allocation of ^{13}C into the epicuticular VLCFAs (Figure 6c) than into VLCFAs of cellular and cuticular pools (Figure 6b) demonstrates that the former are nearly exclusively synthesized for the formation of epicuticular waxes and rapidly exported after elongation.

The composition of the epicuticular fatty acid fraction of the needles shows, in agreement with previous studies (Günthardt-Goerg 1986), that—besides VLCFAs—also mid-chain (16:0) and short-chain (14:0) fatty acids are characteristic for the epicuticular layer of Norway spruce. Interestingly, similar patterns of ^{13}C enrichment of cellular and cuticular fatty acids and of epicuticular ones were detected (Figure 6b and c). This suggests that despite the complex network of biosynthetic pathways and transport mechanisms (Ohlrogge and Browse 1995), similar formation and export rates occur for fatty acids of various chain lengths.

In Norway spruce, besides VLCFAs, major compounds of cuticular waxes include primary alcohols, aldehydes, ketones

and triterpenoids, and alkanes (Samuels et al. 2008, Van Maarseveen et al. 2009). Their abundance depends on leaf development stage. The distribution pattern of the individual alkanes in the cuticle, with a clear dominance of C₂₉ (Figure 6a), was also found in other conifers (Maffei et al. 2004, Zech et al. 2009, Nikolić et al. 2012, 2013). As alkanes are produced from fatty acid precursors in the ER exclusively for export (Samuels et al. 2008), it is logical that the alkane concentration in the cellular and cuticular pool is ~55 times lower than the fatty acid concentration (Figure 3a).

The odd-over-even predominance in the homologous series of the alkanes (Figure 7a) clearly indicates alkane formation by decarbonylation from the respective fatty acid precursors (Bognar et al. 1984, Samuels et al. 2008). Thus, the decreasing ¹³C incorporation into the cellular and cuticular fatty acids 24:0–30:0 (Figure 6b) accounts for a similar decrease in ¹³C incorporation in the cellular and cuticular alkanes with chain lengths from C₂₃ to C₂₉ (Figure 7b). Nevertheless, ¹³C incorporation into epicuticular alkanes (Figure 7c) was measurable even after 6 h, pointing to their rapid de novo synthesis in the ER and subsequent export to detectable levels even after short time periods. This corroborates Kahmen et al. (2011) and Van Maarseveen et al. (2009), who found that wax alkanes are formed rapidly during cuticle development even in very early ontogeny stages of young leaves.

Gao et al. (2012) conducted similar studies of leaf lipid turnover based on deuterium labelling. They found on average 10 times higher regeneration rates (which corresponds to the incorporation in our study) of fatty acids and alkanes for the grass *Phleum pratense*. This observation clearly shows that C allocation and turnover in herbaceous species cannot be compared with woody plants, and that C allocation studies must be performed for individual plant types and growth stages. However, higher turnover based on deuterium labelling could also reflect deuterium exchange during lipid recycling at the terminal, activated positions of the acyl chain (i.e., the C atom, where the Coenzyme A is attached). Therefore, dual-isotope labelling studies combining deuterium and ¹³C labelling are urgently required to enable comparison of metabolic pathway studies based on only one of the two labelling approaches. Nevertheless, some basic metabolic principles seem to be similar: Gao et al. (2012) found a five times higher regeneration rate of VLCFAs compared with precursor fatty acids (16:0 and 18:0) and a 5–10 times higher regeneration rate of VLCFAs compared with the alkanes formed from them. These ratios are similar to the ratios of ¹³C enrichment we found, indicating that basic metabolic principles of lipid metabolism can be investigated by deuterium as well as C isotope labelling.

Conclusions and outlook

This study is, to our knowledge, the first to couple field pulse labelling of entire trees with a detailed tracing of the allocation

of photosynthetically fixed ¹³C into individual substance classes by compound-specific isotope analysis. C allocation several days after bud break is clearly dominated by the investment of freshly assimilated C into direct needle growth. Within the needles, the fast-responding sugar and amino acid pools received the highest ¹³C allocation. Metabolic tracing based on amino acids demonstrated that serine and glycine point to a high photorespiratory activity, phenylalanine to intensive C allocation in secondary metabolism and methionine to a high demand for C-1 groups for methylations required in many important biosynthetic pathways after bud break. The detectable and significant allocation into epicuticular VLCFAs and alkanes 6 h after labelling demonstrates that even complex biosynthetic processes involving many biosynthetic, transformation and transport steps can take place within short periods. ¹³C enrichment did, however, clearly decrease along the biosynthetic pathway of lipid formation with 16:0 and 18:0 precursors > elongated long-chain fatty acids > decarbonylated alkanes. However, ¹³C dynamics in slow-versus fast-cycling pools is dominated by different processes such as net de novo synthesis or degradation of certain tissue compounds. In addition, C allocation towards de novo synthesis can occur not only from freshly assimilated ¹³CO₂ but also from reallocated, old C. This complex network of processes and C sources restricts an unambiguous tracing of C allocation pathways, which would require either sampling at various time intervals after labelling or position-specific labelling of plant metabolites in situ.

Finally, our approach combining in situ pulse labelling with compound-specific ¹³C analysis of key metabolites significantly improves our understanding of C allocation in plant tissues at a certain growth stage and elucidates the underlying metabolic pathways (Figure 1). Both those pathways directly involved in the formation of structural compounds, and many minor pathways (which are side reactions, have regulatory functions or synthesize secondary metabolites) are highly relevant for C allocation during intensive needle growth. For a more detailed reconstruction of metabolic pathways, we suggest (i) extending the structural cellular compounds to include cellulose and lignin precursors, (ii) extending the investigated compounds to include secondary metabolites, e.g., terpenes, especially if conifer metabolism is being investigated and (iii) combining ¹³C with deuterium labelling studies for a more detailed view on lipid metabolism.

Acknowledgments

We gratefully thank Prof. Bernd Huwe for providing laboratories and instrumentation for sample preparation. Furthermore, we thank Iris Schmiedinger (BAYCEER, Laboratory for Isotope Biogeochemistry, University of Bayreuth) and Stefanie Boesel (GC-EA-IRMS Laboratory of the Soil Biogeochemistry, Martin-Luther-University Halle-Wittenberg) for bulk isotope analysis

and support for the compound-specific isotope analysis, respectively.

Conflict of interest

None declared.

Funding

This study was funded by the German Research Foundation (DFG, research unit 562) through Project GL 327/11-1.

References

- Amelung W, Zhang X (2001) Determination of amino acid enantiomers in soils. *Soil Biol Biochem* 33:553–562.
- Amelung W, Cheshire MV, Guggenberger G (1996) Determination of neutral and acidic sugars in soil by capillary gas-liquid chromatography after trifluoroacetic acid hydrolysis. *Soil Biol Biochem* 28: 1631–1639.
- Bao X, Focke M, Pollard M, Ohlrogge J (2000) Understanding in vivo carbon precursor supply for fatty acid synthesis in leaf tissue. *Plant J* 22:39–50.
- Barthel M, Hammerle A, Sturm P, Baur T, Gentsch L, Knohl A (2011) The diel imprint of leaf metabolism on the $\delta^{13}\text{C}$ signal of soil respiration under control and drought conditions. *New Phytol* 192:925–938.
- Biasi C, Pitkämäki AS, Tavi NM, Koponen HT, Martikainen PJ (2012) An isotope approach based on ^{13}C pulse-chase labelling vs. the root trenching method to separate heterotrophic and autotrophic respiration in cultivated peatlands. *Boreal Environ Res* 17:184–192.
- Bognar AL, Paliyath G, Rogers L, Kolattukudy PE (1984) Biosynthesis of alkanes by particulate and solubilized enzyme preparations from pea leaves (*Pisum sativum*). *Arch Biochem Biophys* 235:8–17.
- Brandes E, Kodama N, Whittaker K, Weston C, Rennenberg H, Keitel C, Adams MA, Gessler A (2006) Short-term variation in the isotopic composition of organic matter allocated from the leaves to the stem of *Pinus sylvestris*: effects of photosynthetic and postphotosynthetic carbon isotope fractionation. *Glob Change Biol* 12:1922–1939.
- Brückner H, Westhauser T (2003) Chromatographic determination of L- and D-amino acids in plants. *Amino Acids* 24:43–55.
- Brüggemann N, Gessler A, Kayler Z et al. (2011) Carbon allocation and carbon isotope fluxes in the plant-soil-atmosphere continuum: a review. *Biogeosciences* 8:3457–3489.
- Burget EG, Verma R, Mølhøj M, Reiter W-D (2003) The biosynthesis of L-arabinose in plants: molecular cloning and characterization of a Golgi-localized UDP-D-xylose 4-epimerase encoded by the *MUR4* gene of *Arabidopsis*. *Plant Cell* 15:523–531.
- Conover WJ (1980) *Practical nonparametric statistics*, 2nd edn. Wiley, New York.
- Craig H (1953) The geochemistry of the stable carbon isotopes. *Geochim Cosmochim Acta* 3:53–92.
- Damesin C (2003) Respiration and photosynthesis characteristics of current-year stems of *Fagus sylvatica*: from the seasonal pattern to an annual balance. *New Phytol* 158:465–475.
- Dannoura M, Maillard P, Fresneau C et al. (2011) In situ assessment of the velocity of carbon transfer by tracing ^{13}C in trunk CO_2 efflux after pulse labelling: variations among tree species and seasons. *New Phytol* 190:181–192.
- Dixon RK, Turner DP (1991) The global carbon cycle and climate change: responses and feedbacks from below-ground systems. *Environ Pollut* 73:245–262.
- Ebringerová A (2005) Structural diversity and application potential of hemicelluloses. *Macromol Symp* 232:1–12.
- Epron D, Ngao J, Dannoura M et al. (2011) Seasonal variations of below-ground carbon transfer assessed by in situ ^{13}C pulse labelling of trees. *Biogeosciences* 8:1153–1168.
- Epron D, Bahn M, Derrien D et al. (2012) Pulse-labelling trees to study carbon allocation dynamics: a review of methods, current knowledge and future prospects. *Tree Physiol* 32:776–798.
- Ericsson A (1978) Seasonal changes in translocation of ^{14}C from different age-classes of needles on 20-year-old Scots pine trees (*Pinus sylvestris*). *Physiol Plant* 43:351–358.
- Fischer C, Höll W (1991) Food reserves of Scots pine (*Pinus sylvestris* L.). *Trees* 5:187–195.
- Franceschi VR, Krokene P, Krekling T, Christiansen E (2000) Phloem parenchyma cells are involved in local and distant defense responses to fungal inoculation or bark-beetle attack in Norway spruce (Pinaceae). *Am J Bot* 87:314–326.
- Gall R, Landolt W, Schleppli P, Michellod V, Bucher JB (2002) Water content and bark thickness of Norway spruce (*Picea abies*) stems: phloem water capacitance and xylem sap flow. *Tree Physiol* 22:613–623.
- Gao L, Burnier A, Huang Y (2012) Quantifying instantaneous regeneration rates of plant leaf waxes using stable hydrogen isotope labeling. *Rapid Commun Mass Spectrom* 26:115–122.
- Gaspar Y, Johnson KL, McKenna JA, Bacic A, Schultz CJ (2001) The complex structures of arabinogalactan-proteins and the journey towards understanding function. *Plant Mol Biol* 47:161–176.
- Gearing JN (1991) The study of diet and trophic relationships through natural abundance of carbon-13. In: Coleman DC, Fry B (eds) *Carbon isotope techniques*. Academic Press, Inc., San Diego, CA, USA, pp 201–218.
- Gessler A, Rennenberg H, Keitel C (2004) Stable isotope composition of organic compounds transported in the phloem of European beech—evaluation of different methods of phloem sap collection and assessment of gradients in carbon isotope composition during leaf-to-stem transport. *Plant Biol* 6:721–729.
- Ghirardo A, Koch K, Taipale R, Zimmer INA, Schnitzler J-P, Rinne J (2010) Determination of de novo and pool emissions of terpenes from four common boreal/alpine trees by ^{13}C labelling and PTR-MS analysis. *Plant Cell Environ* 33:781–792.
- Glaser B, Amelung W (2002) Determination of ^{13}C natural abundance of amino acid enantiomers in soil: methodological considerations and first results. *Rapid Commun Mass Spectrom* 16:891–898.
- Glaser B, Benesch M, Dippold M, Zech W (2012) In situ ^{15}N and ^{13}C labelling of indigenous and plantation tree species in a tropical mountain forest (Munessa, Ethiopia) for subsequent litter and soil organic matter turnover studies. *Org Geochem* 42:1461–1469.
- Gunina A, Dippold MA, Glaser B, Kuzyakov Y (2014) Fate of low molecular weight organic substances in an arable soil: from microbial uptake to utilisation and stabilisation. *Soil Biol Biochem* 77:304–313.
- Günthardt-Goerg MS (1986) Epicuticular wax of needles of *Pinus cembra*, *Pinus sylvestris* and *Picea abies*. *Eur J For Pathol* 16:400–408.
- Hansen J, Beck E (1994) Seasonal changes in the utilization and turnover of assimilation products in 8-year-old Scots pine (*Pinus sylvestris* L.) trees. *Trees* 8:172–182.
- Hansen J, Vogg G, Beck E (1996) Assimilation, allocation and utilization of carbon by 3-year-old Scots pine (*Pinus sylvestris* L.) trees during winter and early spring. *Trees* 11:83–90.
- Harwood JL, Russell NJ (1984) *Lipids in plants and microbes*. George Allen & Unwin, London.
- Heldt H-W, Piechulla B (2008) *Pflanzenbiochemie*. Spektrum Akademischer, Heidelberg.
- Herschbach C, Gessler A, Rennenberg H (2012) Long-distance transport and plant internal cycling of N- and S-compounds. In: Lüttge U, Beyschlag W, Büdel B, Francis D (eds) *Progress in botany*, Vol. 73. Springer, Berlin, Heidelberg, pp 161–188.

- Hoch G, Popp M, Körner C (2002) Altitudinal increase of mobile carbon pools in *Pinus cembra* suggests sink limitation of growth at the Swiss treeline. *Oikos* 98:361–374.
- Hoch G, Richter A, Körner C (2003) Non-structural carbon compounds in temperate forest trees. *Plant Cell Environ* 26:1067–1081.
- Högberg P, Nordgren A, Buchmann N, Taylor AFS, Ekblad A, Högberg MN, Nyberg G, Ottosson-Löfvenius M, Read DJ (2001) Large-scale forest girdling shows that current photosynthesis drives soil respiration. *Nature* 411:789–792.
- Hurlock AK, Roston RL, Wang K, Benning C (2014) Lipid trafficking in plant cells. *Traffic* 15:915–932.
- IUSS Working Group WRB (2014) World reference base for soil resources (2014). *World Soil Resources Reports* 106. FAO, Rome.
- Jansen K, Du B, Kayler Z et al. (2014) Douglas-fir seedlings exhibit metabolic responses to increased temperature and atmospheric drought. *PLoS One* 9:e114165. doi:10.1371/journal.pone.0114165
- Jetter R, Schäffer S, Riederer M (2000) Leaf cuticular waxes are arranged in chemically and mechanically distinct layers: evidence from *Prunus laurocerasus* L. *Plant Cell Environ* 23:619–628.
- Kagawa A, Sugimoto A, Maximov TC (2006) Seasonal course of translocation, storage and remobilization of ^{13}C pulse-labeled photoassimilate in naturally growing *Larix gmelinii* saplings. *New Phytol* 171:793–804.
- Kahmen A, Dawson TE, Vieth A, Sachse D (2011) Leaf wax *n*-alkane δD values are determined early in the ontogeny of *Populus trichocarpa* leaves when grown under controlled environmental conditions. *Plant Cell Environ* 34:1639–1651.
- Keel SG, Siegwolf RTW, Körner C (2006) Canopy CO_2 enrichment permits tracing the fate of recently assimilated carbon in a mature deciduous forest. *New Phytol* 172:319–329.
- Keel SG, Campbell CD, Högberg MN et al. (2012) Allocation of carbon to fine root compounds and their residence times in a boreal forest depend on root size class and season. *New Phytol* 194:972–981.
- Kolattukudy PE (1970) Biosynthesis of cuticular lipids. *Annu Rev Plant Physiol* 21:163–192.
- Konôpka B, Yuste JC, Janssens IA, Ceulemans R (2005) Comparison of fine root dynamics in Scots pine and pedunculate oak in sandy soil. *Plant Soil* 276:33–45.
- Körner C (2003) Carbon limitation in trees. *J Ecol* 91:4–17.
- Kreyling J, Wiesenberg GLB, Thiel D, Wohlfart C, Huber G, Walter J, Jentsch A, Konnert M, Beierkuhnlein C (2012) Cold hardiness of *Pinus nigra* Arnold as influenced by geographic origin, warming, and extreme summer drought. *Environ Exp Bot* 78:99–108.
- Kuptz D, Fleischmann F, Matyssek R, Grams TEE (2011) Seasonal patterns of carbon allocation to respiratory pools in 60-yr-old deciduous (*Fagus sylvatica*) and evergreen (*Picea abies*) trees assessed via whole-tree stable carbon isotope labeling. *New Phytol* 191:160–172.
- Kuzyakov Y, Domanski G (2000) Carbon input by plants into the soil. *Review. J Plant Nutr Soil Sci* 163:421–431.
- Kuzyakov Y, Gavrichkova O (2010) REVIEW: time lag between photosynthesis and carbon dioxide efflux from soil: a review of mechanisms and controls. *Glob Change Biol* 16:3386–3406.
- Li-Beisson Y, Shorrosh B, Beisson F et al. (2013) Acyl-lipid metabolism. *Arabidopsis Book* 11:e0161.
- Lippu J (1994) Patterns of dry matter partitioning and ^{14}C -photosynthate allocation in 1.5-year-old Scots pine seedlings. *Silva Fenn* 28:145–153.
- Maffei M, Badino S, Bossi S (2004) Chemotaxonomic significance of leaf wax *n*-alkanes in the *Pinales* (Coniferales). *J Biol Res* 1:3–19.
- Malhi Y, Baldocchi DD, Jarvis PG (1999) The carbon balance of tropical, temperate and boreal forests. *Plant Cell Environ* 22:715–740.
- Markham JE, Molino D, Gissot L et al. (2011) Sphingolipids containing very-long-chain fatty acids define a secretory pathway for specific polar plasma membrane protein targeting in *Arabidopsis*. *Plant Cell* 23:2362–2378.
- Moroney JV, Jungnick N, DiMario RJ, Longstreth DJ (2013) Photorespiration and carbon concentrating mechanisms: two adaptations to high O_2 , low CO_2 conditions. *Photosynth Res* 117:121–131.
- Nikolić B, Tešević V, Dorđević I, Todosijević M, Jadrnanin M, Bojović S, Marin PD (2012) Chemodiversity of nonacosan-10-ol and *n*-alkanes in the needle wax of *Pinus heldreichii*. *Chem Biodivers* 9:80–90.
- Nikolić B, Tešević V, Dorđević I, Todosijević M, Jadrnanin M, Bojović S, Marin PD (2013) Variability of *n*-alkanes and nonacosan-10-ol in natural populations of *Picea omorika*. *Chem Biodivers* 10:473–483.
- Nogués S, Damesin C, Tcherkez G, Maunoury F, Cornic G, Ghashghaie J (2006) $^{13}\text{C}/^{12}\text{C}$ isotope labelling to study leaf carbon respiration and allocation in twigs of field-grown beech trees. *Rapid Commun Mass Spectrom* 20:219–226.
- Ohlroge J, Browse J (1995) Lipid biosynthesis. *Plant Cell* 7:957–970.
- Plain C, Gerant D, Maillard P, Dannoura M, Dong Y, Zeller B, Priault P, Parent F, Epron D (2009) Tracing of recently assimilated carbon in respiration at high temporal resolution in the field with a tuneable diode laser absorption spectrometer after in situ $^{13}\text{CO}_2$ pulse labelling of 20-year-old beech trees. *Tree Physiol* 29:1433–1445.
- Priault P, Wegener F, Werner C (2009) Pronounced differences in diurnal variation of carbon isotope composition of leaf respired CO_2 among functional groups. *New Phytol* 181:400–412.
- Prügel B, Lognay G (1996) Composition of the cuticular waxes of *Picea abies* and *P. sitchensis*. *Phytochem Anal* 7:29–36.
- Pumpanen JS, Heinonsalo J, Rasilo T, Hurme K-R, Ilvesniemi H (2009) Carbon balance and allocation of assimilated CO_2 in Scots pine, Norway spruce, and Silver birch seedlings determined with gas exchange measurements and ^{14}C pulse labelling. *Trees* 23:611–621.
- Renault S, Zwiazek JJ (1997) Cell wall composition and elasticity of dormant and growing white spruce (*Picea glauca*) seedlings. *Physiol Plant* 101:323–327.
- Richardson AD, Carbone MS, Keenan TF, Czimczik CI, Hollinger DY, Murakami P, Schaberg PG, Xu X (2013) Seasonal dynamics and age of stemwood nonstructural carbohydrates in temperate forest trees. *New Phytol* 197:850–861.
- Riikonen J, Kontunen-Soppela S, Ossipov V, Tervahauta A, Tuomainen M, Oksanen E, Vapaavuori E, Heinonen J, Kivimäenpää M (2012) Needle metabolome, freezing tolerance and gas exchange in Norway spruce seedlings exposed to elevated temperature and ozone concentration. *Tree Physiol* 32:1102–1112.
- Samuels L, Kunst L, Jetter R (2008) Sealing plant surfaces: cuticular wax formation by epidermal cells. *Annu Rev Plant Biol* 59:683–707.
- Sangster A, Knight D, Farrell R, Bedard-Haughn A (2010) Repeat-pulse $^{13}\text{CO}_2$ labeling of canola and field pea: implications for soil organic matter studies. *Rapid Commun Mass Spectrom* 24:2791–2798.
- Sauheitl L, Glaser B, Bol R (2005) Short-term dynamics of slurry-derived plant and microbial sugars in a temperate grassland soil as assessed by compound-specific $\delta^{13}\text{C}$ analyses. *Rapid Commun Mass Spectrom* 19:1437–1446.
- Sauheitl L, Glaser B, Weigelt A (2009) Advantages of compound-specific stable isotope measurements over bulk measurements in studies on plant uptake of intact amino acids. *Rapid Commun Mass Spectrom* 23:3333–3342.
- Schädel C, Blöchl A, Richter A, Hoch G (2009) Short-term dynamics of nonstructural carbohydrates and hemicelluloses in young branches of temperate forest trees during bud break. *Tree Physiol* 29:901–911.
- Springer U, Lehner A (1952) Stoffabbau und Humusaufbau bei der aeroben und anaeroben Zersetzung landwirtschaftlich und forstwirtschaftlich wichtiger organischer Stoffe I. *Z Pflanzenernähr Düng Bodenkd* 58:193–231.
- Streit K, Rinne KT, Hagedorn F, Dawes MA, Saurer M, Hoch G, Werner RA, Buchmann N, Siegwolf RTW (2013) Tracing fresh assimilates through

- Larix decidua* exposed to elevated CO₂ and soil warming at the alpine treeline using compound-specific stable isotope analysis. *New Phytol* 197:838–849.
- Timell TE (1967) Recent progress in the chemistry of wood hemicelluloses. *Wood Sci Technol* 1:45–70.
- Trumbore S (2006) Carbon respired by terrestrial ecosystems—recent progress and challenges. *Glob Change Biol* 12:141–153.
- van Dongen BE, Schouten S, Damsté JSS (2001) Gas chromatography/combustion/isotope-ratio-monitoring mass spectrometric analysis of methylboronic derivatives of monosaccharides: a new method for determining natural ¹³C abundances of carbohydrates. *Rapid Commun Mass Spectrom* 15:496–500.
- Van Maarseveen C, Han H, Jetter R (2009) Development of the cuticular wax during growth of *Kalanchoe daigremontiana* (Hamet et Perr. de la Bathie) leaves. *Plant Cell Environ* 32:73–81.
- Vogt T (2010) Phenylpropanoid biosynthesis. *Mol Plant* 3:2–20.
- Wiesenberg GLB, Gocke M, Kuzyakov Y (2010) Fast incorporation of root-derived lipids and fatty acids into soil—evidence from a short term multiple pulse labelling experiment. *Org Geochem* 41:1049–1055.
- Wirtz M, Droux M (2005) Synthesis of the sulfur amino acids: cysteine and methionine. *Photosynth Res* 86:345–362.
- Würth MKR, Peláez-Riedl S, Wright SJ, Körner C (2005) Non-structural carbohydrate pools in a tropical forest. *Oecologia* 143:11–24.
- You L, Page L, Feng X, Berla B, Pakrasi HB, Tang YJ (2012) Metabolic pathway confirmation and discovery through ¹³C-labeling of proteino-genic amino acids. *J Vis Exp* 59:e3583.
- Zech M, Glaser B (2008) Improved compound-specific δ¹³C analysis of n-alkanes for application in palaeoenvironmental studies. *Rapid Commun Mass Spectrom* 22:135–142.
- Zech M, Buggle B, Leiber K et al. (2009) Reconstructing Quaternary vegetation history in the Carpathian Basin, SE Europe, using n-alkane biomarkers as molecular fossils. *Quat Sci J* 58:148–155.